Asian Journal of Chemistry; Vol. 28, No. 10 (2016), 2131-2138

ASIAN JOURNAL OF CHEMISTRY

http://dx.doi.org/10.14233/ajchem.2016.19885

Kinetics and Equilibrium Studies of Pb^{2+}, Zn^{2+} and Cd^{2+} Adsorption onto Activated Carbon from Breadnut Seed Shell

O.C. OKPAREKE[1,2,*], P.M. EJIKEME[1] and J.C. IGWE[3]

[1]Physical Chemistry Unit, Department of Pure and Industrial Chemistry, University of Nigeria, Nsukka, Nigeria
[2]Department of Chemistry, Faculty of Science and Engineering, University of Waikato, Hamilton, New Zealand
[3]Department of Industrial Chemistry, Abia State University, Uturu, Nigeria

*Corresponding author: E-mail: obinna.okpareke@unn.edu.ng

Received: 3 February 2016; *Accepted*: 13 May 2016; *Published online*: 30 June 2016; AJC-17955

Activated carbon from breadnut shell was prepared and characterized by FTIR, SEM, EDS and BET nitrogen-adsorption surface area and pore volume measurements. The activated carbon was used to study the mechanism of the removal of Pb^{2+}, Zn^{2+} and Cd^{2+} from aqueous solution. The effect of pH, temperature, contact time, metal ion concentration and adsorbent loading on the sorption process was investigated. Batch adsorption studies were carried out at room temperature. BET measurements gave a remarkably high surface area (911.2 m^2/g) and a total pore volume of 0.008 m^2/g. The efficiency of metal ion uptake was found to be dependent on the pH with maximum adsorption at pH between 5.5 and 6.0. The amount of metal ion adsorbed increased with increase in temperature, adsorbent loading, initial metal ion concentration and contact time. Equilibrium was attained after 150 min and the maximum adsorption was achieved at an adsorbent loading of 1.2 g/500 mL metal ion solution. The metal uptake capacity followed the trend $Cd^{2+} > Pb^{2+} > Zn^{2+}$. The kinetic studies for the sorption process showed rapid sorption dynamics by a pseudo second order model. Equilibrium isotherms were analyzed by the Langmuir and Freundlich adsorption isotherm models and the adsorption equilibrium data showed that Pb^{2+}adsorption fitted well to the Langmuir model, while Zn^{2+} and Cd^{2+} was better fitted to the Freundlich adsorption model.

Keywords: Activated carbon, Kinetics, Sorption, Breadnut seed shell, Heavy metal removal.

INTRODUCTION

The increased awareness on water pollution implies that studies concerning water treatment and industrial wastewater remediation are of primary importance. Industrial and technological expansion, energy utilization and half hazard rapid urbanization have rendered many water bodies unwholesome, due to the indiscriminate disposal of heavy metal containing effluents into these water bodies. Most of these metal ions which include copper, lead, chromium, zinc, mercury, nickel, cadmium and iron are toxic to humans and the ecological environment. A number of technologies have been developed over the years to remove heavy metals from industrial wastewater [1]. The most important technologies include coagulation and flocculation [2,3]. Other conventional methods such as precipitation, ion exchange, electrochemical processes and membrane technology have also been explored [4,5]. However disadvantages like incomplete removal, high reagent cost, high energy needs and generation of toxic waste products that need careful disposal has made it imperative to develop new and cost effective methods of removing heavy metals from wastewater [6]. Adsorption has been widely accepted in environmental treatment applications around the world today. Liquid-solid state adsorption systems are based on the ability of certain solids to preferentially concentrate specific substances from solutions onto their surfaces. This principle can be applied for the removal of various pollutants from industrial wastewater. Recently a lot of research effort has been geared towards the application of natural, low cost, high capacity adsorbents for the removal of metal ions from aqueous solution [7-11]. A wide range of adsorbents have been prepared and tested, including several agricultural by-products [8,11] and a good number of activated carbonaceous materials [9,10,12]. Other low cost adsorbents such as fly ash and clay [13,14] have also been applied in heavy metal remediation from aqueous solution. The use of naturally occurring minerals such as coal, calcium bentonite and bone char with potential for adsorption of heavy metals have also been reported [15-17]. The present effort is aimed at the preparation of a low cost, high capacity activated carbon from Breadnut shell, an agricultural waste for the removal of Pb^{2+}, Cd^{2+} and Zn^{2+} from aqueous solution.

EXPERIMENTAL

The absorbance values were measured with a Varian AA1275 model atomic absorption spectrophotometer (AAS). pH was measured with a pH-meter (Jenway 3010) and Thermostated Reciprocating Shaker (Nuvet ST 400) was used for sample agitation during adsorption experiments. Infrared spectral analysis was performed on the Perkin Elmer spectrum 100 FT-IR spectrometer. The microstructure and surface characteristics of the adsorbents was analyzed on a Hitachi S-4700 SEM, while the surface area and pore size analysis was carried out on the Quantachrome Nova 2200e surface area and pore size analyser using the BET adsorption method at liquid nitrogen temperature. The elemental components of the breadnut activated carbon adsorbent were determined by energy dispersive X-ray spectroscopy.

Adsorbent: Breadnut (*Artocarpus altitis)* is a tropical flowering food plant grown in Nigeria and other parts of Africa. The seed shells, an agricultural waste of no known value were collected from Ogige main market in Nsukka area of Enugu State, Nigeria. The shells were washed with water to remove the fluffy part and any adhering dirt particles. The shells were sun-dried, pulverized and stored in a desiccator for further use.

Carbonization and activation: About 200 g of the dried precursor was carbonized in a muffle furnace at 400 °C for 0.5 h under purified nitrogen flow. The carbonized material (120 g) was weighed into a crucible containing 120 g of potassium hydroxide dissolved in distilled water. The paste like material was allowed to stand for 1 h and was heated to boil. The crucible was later placed in a muffle furnace and the sample activated for about 1 h at 500 °C. The crucible and its contents was withdrawn and allowed to cool. The resultant activated carbon was then washed sequentially with 0.1 M HCl and then with deionized water until washing solution reached a pH of about 7. The activated carbonaceous material was dried in an oven at 105 °C, stored in a desiccator and labelled breadnut activated carbon.

Adsorbate: Equivalent amounts of analytical grade $ZnSO_4$, $PbNO_3$ and $CdSO_4 \cdot 7H_2O$ obtained from Sigma Aldrich Ltd. were dissolved in distilled water. 1000 mg/L of stock solution was prepared and working solutions were gotten by successive dilutions. The pH of the solution was adjusted to the required value using 0.1 M HCl and 0.1 M NaOH solutions.

Batch adsorption experiments: Batch experiments were performed at 30 ± 2 °C in a 250 mL flask containing 150 mL metal ion solution and shaken in a thermostated reciprocating shaker at 125-150 strokes/min. The effect of pH on the adsorption capacity was studied by varying the pH of the metal ion solution between 2 and 8 in a 150 mL metal ion solution of 300 mg/L concentration at 30 °C and constant time of 180 min. The pH of the metal ion solutions were adjusted by adding 0.1 M HCl or NaOH solutions. The effect of adsorbent dosage was investigated by using different weights of adsorbent (0.2-1.2 g per 150 mL) while keeping the concentration of metal ion and other parameters constant. The effect of contact time on the removal efficiency of the adsorbents was also studied by varying the contact time between 5 and 180 min at constant temperature of 30 °C in different experimental runs. The amount of metal ions adsorbed at different temperatures was also investigated by varying the temperature of the metal ion solution between 20 and 80 °C. The sorption capacity of the adsorbent for the different metal ions at varying initial concentrations (100-500 mg/L) prepared from stock solutions at constant pH and temperature was investigated. The equilibrium concentrations of the metal ions (Ce) was determined by atomic absorption spectrophotometry (AAS). The amount of metal ion adsorbed per unit gram of adsorbent q(mg/g) and the sorption efficiency E were calculated using eqns. 1 and 2 [18]:

$$q = \frac{C_i - C_f}{m} \times V \quad (1)$$

$$E = \frac{C_i - C_f}{C_i} \times 100 \quad (2)$$

where C_i is the initial metal ion concentration and C_f is the final metal ion concentration. m is the mass of the adsorbent, V is the volume of the reaction mixture in mL and E is the removal efficiency.

RESULTS AND DISCUSSION

Characterization and physiochemical properties of breadnut activated carbon (BAC): The physical and chemical characteristics of activated carbon prepared from bread fruit nut shell is presented in Table-1.

TABLE-1
PHYSICO-CHEMICAL CHARACTERISTICS OF THE ACTIVATED CARBON

S. No.	Parameters	Values
1	Surface area (m^2/g)	911.2
2	pH	7.4
3	Ash content (%)	9.4
4	Pore volume (m^3/g)	0.008
5	Bulk density (g/mL)	0.345
6	Decolourizing power (%)	99.84
7	Moisture content (%)	12.01
8	Carbon yield (%)	39.966
9	Energy value (J/g)	2142.40
10	Conductivity (μs)	250

The surface area and pore characteristics of the breadnut activated carbon is shown in Table-1. The BET surface area and total pore volume of breadnut activated carbon were recorded as 911.2 and 0.008 m^2/g, respectively. These values are comparable with the commercial F300 and F400 AC from Merck [19], which were reported to have BET surface area of 957 and 960 m^2/g and total pore volume 0.525 and 0.56 cm^3/g, respectively. It is clear from the table that the adsorbent exhibited high surface area as well as decolourizing power. The moisture content of the breadnut activated carbon (12.01 %) is indicative of its hydrophilic nature.

Infrared spectral analysis: The infrared spectral data of the breadnut activated carbon (BAC) before adsorption is shown in Fig. 1a and interpretation of the relevant spectral bands are also shown in Table-2. The weak broad absorption bands at 3798 cm^{-1} has been attributed to ν(O-H) of the phenolic and aliphatic groups or surface bonded water or N-H stretching

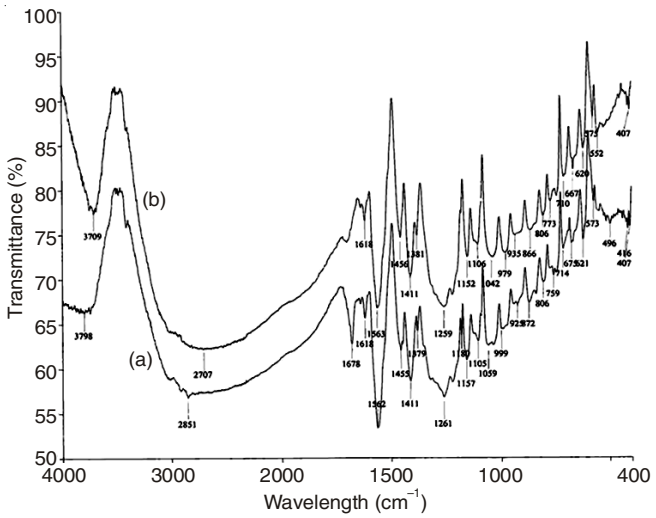

Fig. 1. FT-IR spectra of (a) breadnut activated carbon before and (b) breadnut activated carbon after adsorption

TABLE-2
FOURIER TRANSFORM INFRARED SPECTRAL DATA FOR ACTIVATED CARBON FROM BREAD FRUIT NUT SHELL

FTIR peaks (cm^{-1})	Assignments
3798	ν(OH) of H_2O (phenolic and aliphatic groups) or N-H stretching
2851	C-H stretching (methyl, methylene groups)
1678	C=O and C=C (carbonyl)
1618	N-H bending vibrations
1562	C-N stretching
1411	C-H bending
1379	ν(C-O) (carboxylate group)
1261	C-N vibrations (aromatic groups)
1059	C-O-C stretching (ether group in carbohydrates)

frequency of amido and amino groups [20]. The band at 2851 cm^{-1} has been assigned to C-H stretching of methylene and methoxy groups on the surface of the adsorbent, while the medium bands at 1678 and 1618 cm^{-1} has been attributed to carbonyl stretching frequencies of the unsaturated aliphatic aldehydic groups and N-H bending vibrations of aromatic groups, respectively. The very strong bands at 1562 cm^{-1} has been assigned to C=N stretching frequencies of diimides, while the band at 1455 and 1379 cm^{-1} has been attributed to C-H bending and ν(C-O) vibration of the carboxylate groups, respectively [21]. The bands at 1261 and 1157 cm^{-1} has been assigned to C-N vibrations of aromatic and aliphatic groups. The infrared characterization of the adsorbent has shown the presence of many functional groups capable of binding to metal cations. The infrared spectrum of the breadnut activated carbon adsorbent impregnated with metal ions after adsorption has been shown (Fig. 1b). The FT-IR spectrum when compared with that of the free breadnut activated carbon shows that some peaks shifted or disappeared and new peaks were detected indicating the possible involvement of those functional groups on the surface of breadnut activated carbon in the metal binding process.

Surface characterization: The morphology and surface characteristics of the carbonaceous materials were studied with the aid of the SEM [22]. The SEM micrographs for breadnut activated carbon adsorbent before and after metal ion adsorption is presented in Fig. 2. The SEM micrographs of the free breadnut activated carbon (Fig. 2a) shows the presence of irregular surface and large heterogeneous layer of pores on the surface of the adsorbents for the uptake of metal ions and the surface of the metal ion loaded breadnut activated carbon (Fig. 2b) clearly shows that the surface and pores has been taken up by metal ions. It is evident from Fig 2b that the dense porous morphology (Fig. 2a) got disturbed after adsorption of metal ions on the adsorbent surface [18].

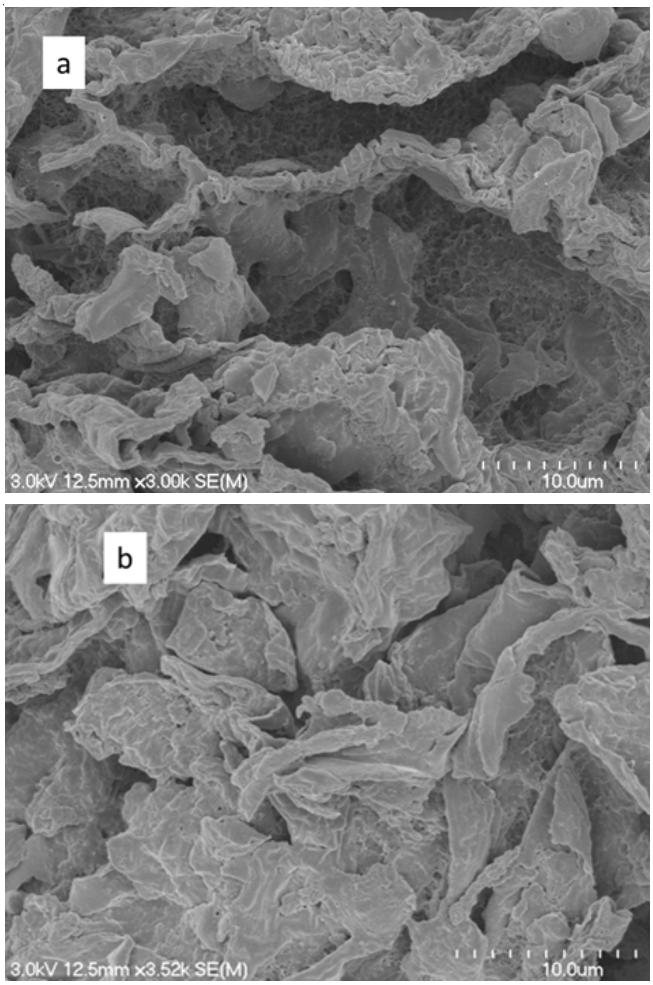

Fig. 2. SEM micrograph of breadnut activated carbon (a) before adsorption and (b) after adsorption

Elemental composition: The elemental analysis for breadnut activated carbon was performed and the results are presented in Table-3. The data shows the presence of different cations on the surface of the adsorbents. The presence of these ions on the adsorbent surface is assumed to have contributed to the high adsorption capacity of the breadnut activated carbon through ion exchange, chelation or complexation reactions [23]. This technique unequivocally showed that carbon was the predominant element as would be expected in a lignocellulose material that has undergone activation and carbonization.

Effect of pH: pH has been identified as a very important controlling factor in the process of adsorption, as it affects the surface charge of the adsorbents and thus the degree of ionization [24]. The efficiency of metal ion removal by the

TABLE-3
ELEMENTAL COMPOSITION OF
BREADNUT ACTIVATED CARBON

S. No.	Element	Composition (%)
1	Carbon	81.43
2	Hydrogen	12.90
3	Magnesium	0.4
4	Potassium	3.68
5	Calcium	1.51

adsorbents was observed to be dependent on the pH of the reaction mixture. Fig. 3 indicates that at very low pH (2-3) the sorption capacity was low, exhibiting maximum adsorption value of 102.67 mg/g (34.22 %) 129.16 mg/g (43.07 %) and 109.12 mg/g (36.36 %) for Zn^{2+}, Cd^{2+} and Pb^{2+} ions, respectively. This observation has been attributed to the protonation of the adsorbent, the development of overall positive charge on the surfaces and the consequent electrostatic repulsive forces on the metal cations [24] as a result of the presence of more H^+ ions. These excess H^+ ions compete with the metal ions for adsorption sites on the surface of the adsorbent, thus reducing the rate of uptake of the metal ions onto the activated carbon. The sorption capacity of the adsorbents increased as the pH of the solution increased, reaching a maximum at pH of 6 with sorption capacity of 259.18 mg/g (87.22 %), 269.12 mg/g (86.39 %) and 269.12 mg/g (89.69 %) for Zn^{2+}, Cd^{2+} and Pb^{2+} ions, respectively, showing more than 100 % increase in adsorption. At pH above 6, sorption capacity was noticed to have declined. This has been attributed to the fact that at higher pH ranges, there is existence of counter ions which might lead to competition for adsorption site, thus lowering the sorption efficiency. It has also been reported that above certain pH range (around 7) that there is a tendency for the precipitation of metal hydroxides on the surface of the adsorbents, thus reducing the number of sites available for metal adsorption [18,24-26].

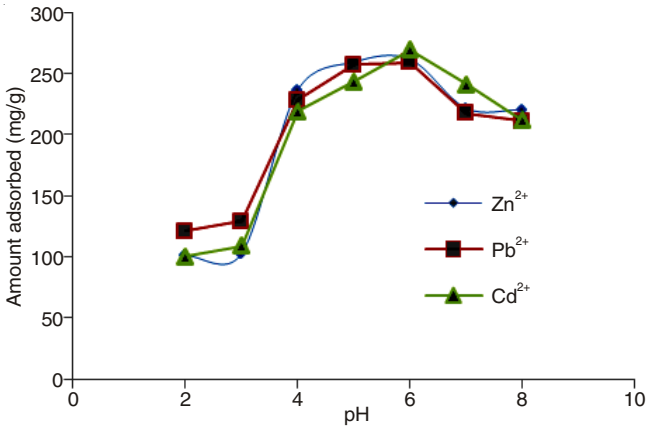

Fig. 3. Graph of amount of metal ion adsorbed at different pH

Effect of adsorbent loading: A study of the effect of adsorbent loading on the adsorption of metal ions onto breadnut activated carbon gives an idea of the effectiveness of the adsorbent and the ability of the metal ions to be adsorbed with a minimum dosage [25,27]. This was investigated by varying the adsorbent loading between 0.2 and 1. 2 mg in a 150 mL of metal ion solution containing 300 mg/L of the metal ions at 30 °C and at a constant pH of 6 and a time of 180 min. The graph of effect of adsorbent weight on the adsorption capacity is shown in Fig. 4. It can be inferred from the charts that there was an increase in sorption as the adsorbent weight increased. This has been attributed to the increase in surface area and the availability of more adsorption sites at higher dose of adsorbents [28]. This result is in agreement with the results of previous studies on some other adsorbents [4,28,29].

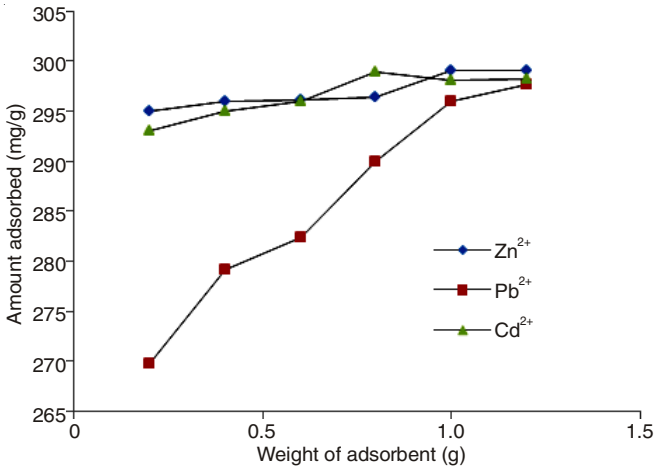

Fig. 4. Graph of amount adsorbed at different adsorbent weight

Effect of temperature: The amount of metal ions adsorbed at different temperature values was investigated by varying the temperature between 20 and 80 °C at a constant pH of 6 and sorption time of 120 min using 150 mL of 300 mg/L metal ion solution. Fig. 5 indicates that the amount of metal ion adsorbed increased slightly with increasing temperature for the metal ions as was also reported for Cr, Hg and As in separate studies by Di Natalie and co-workers [30-32]. This observation depicts an endothermic sorption process in apparent contradiction to the exothermic character of adsorption processes [32].This may be due to the enlargement of the adsorbent pore size on activation of the adsorbent surface at higher temperature values, thus leading to a higher interaction of the metal ions with adsorbent surface. However, the inability to clarify whether the increase in adsorption capacity with temperature was related to either kinetic effects resulting from increased ion diffusivities or due to the "activation" of new adsorption sites on the adsorbent surface or better still to the evolution of sorbent porosity at higher temperature, led us to the classify the overall

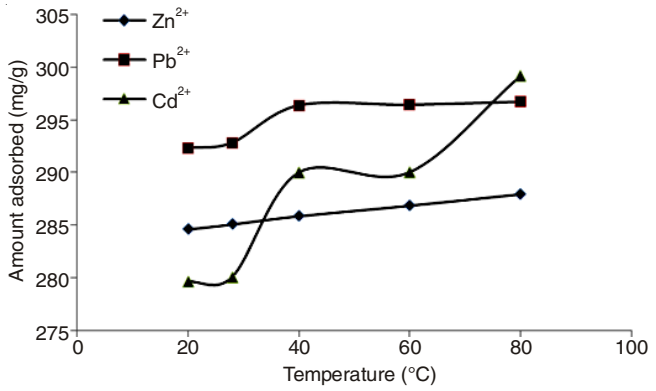

Fig. 5. Graph of amount adsorbed at different temperatures

adsorption process as being apparently endothermic. Albadarin *et al.* [33] and Hu *et al.* [34] reported a contrary result to our observation; a decrease in adsorption with increase in temperature.

Effect of contact time: Fig. 6 shows the effect of contact time on the uptake capacity of studied metal ions onto breadnut activated carbon. The charts indicate a sharp increase in metal uptake within the first 5 min and a gradual uptake afterwards to a maximum at 180 min. Equilibrium sorption was attained at 120 min for Cd^{2+} while Zn^{2+} and Pb^{2+} attained equilibrium at 150 min. These results suggest that the uptake of metal ions may have taken place in phases. The first phase involving the speedy uptake of metal ions as a result of the availability of initial large number of vacant surface active sites. The second phase involves the slow filling of vacant sites due to repulsive forces between the metal ions adsorbed on the breadnut activated carbon surface and the ones from the solution coupled with the difficulty in the diffusion of the metal ions into the intra-particle pores of the adsorbents [24] or the involvement of other mechanisms such as complexation, micro-precipitation and binding site saturation [8,35].

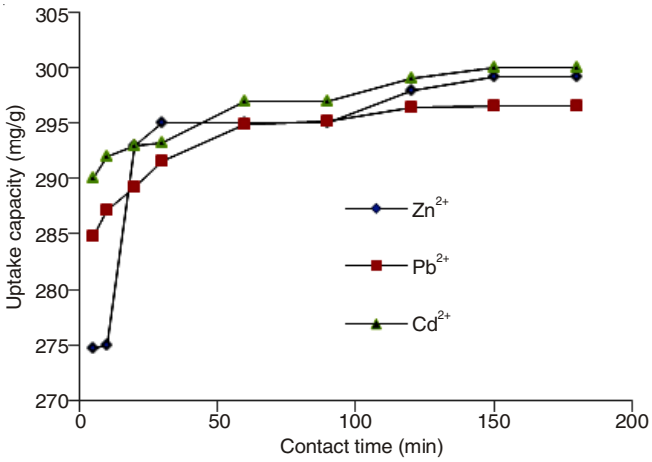

Fig. 6. Graph of uptake capacity against time

Kinetic studies: Kinetic parameters of linear pseudo-first and second order equations were applied to model the adsorption rate of the metal ions onto the activated carbon.

Pseudo-first order model: The pseudo-first order rate expression popularly known as the Langergren equation is generally described by eqn. 3.

$$\frac{dq_t}{dt} = k_a(q_e - q_t) \quad (3)$$

where q_e is the amount of metal ions adsorbed at equilibrium per unit weight of the adsorbent (mg/g) and q is the amount of metal ions adsorbed at any time (mg/g). K_{ad} is the rate constant (min^{-1}). By integrating and applying boundary conditions, $q_t = 0$ at $t = 0$ and to $t = t$ and $q_t = q_t$, at $t = t$, eqn. 3 is linearized to eqn. 4.

$$\ln(q_e - q_t) = \ln(q_e - k_a dt) \quad (4)$$

In order to obtain the rate constants, plots of ln ($q_e - q_t$) against time (t) were made for the three metal ions and they gave fairly straight lines for removal of the three metal ions from aqueous solution (Fig. 7). The pseudo-first order rate parameters were calculated and presented in Table-4.

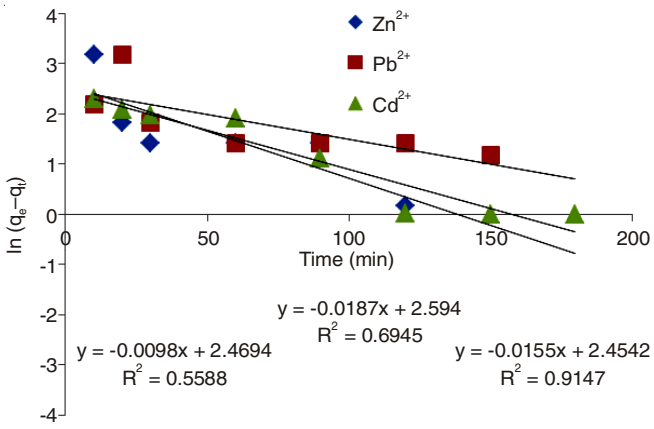

Fig. 7. Pseudo-first order kinetics chart for Zn^{2+}, Cd^{2+} and Pb^{2+} ions

TABLE-4
PSEUDO-FIRST ORDER RATE CONSTANTS

Metal ions	q_e exp (mg/g)	K_{ad} (min^{-1})	q_e cal (mg/g)	R^2
Zn^{2+}	299.11	0.018	13.380	0.694
Pb^{2+}	296.57	0.009	11.810	0.558
Cd^{2+}	299.90	0.015	11.640	0.914

The values of the rate constants presented in Table-4 followed the trend $Zn^{2+} > Cd^{2+} > Pb^{2+}$ which indicates higher rate of adsorption for Zn^{2+} followed by Cd^{2+} and then Pb^{2+}. However the values of the intercept for the three metal ions does not equal the natural logarithm of the equilibrium uptake, coupled with the low R^2 values, thus the adsorption process is not likely to be pseudo-first order dependent [12,36].

Pseudo-second order kinetic model: The adsorption data was also modelled using the pseudo-second order kinetic model represented in eqn. 5 and the linearized form in eqn. 6:

$$\frac{dq_t}{dt} = k_2(q_e - q_t)^2 \quad (5)$$

where K_2 is pseudo-second order rate constant (mg/g min^{-1}). Integrating equation 5 and applying boundary conditions, t = 0 for q = 0 and t = t for q = q_t [37] gives eqn. 6:

$$\frac{t}{q_t} = \frac{1}{k_2 q_e^2} + \frac{1}{q_e}t \quad (6)$$

where $k_2q_e^2 = h_o$, which is the initial adsorption rate. If second order kinetics is applicable, the plot of t/q against t should give a linear relationship from which the constants q_e and h_o can be determined. The pseudo second order kinetic plots are shown in Fig 8 for Zn^{2+}, Cd^{2+} and Pb^{2+} ions. The plots gave good fits to the experimental data, especially with R^2 for Pb equal to unity and R^2 values (Table-5) for Zn and Cd ions close to unity. These results indicate that the adsorption process fitted into the pseudo- second order rate equation. Hence the second order rate constants were evaluated for the three metal ions and also presented in Table-5.The calculated q_e values agreed closely with the experimental data which suggest that the limiting step for the metal ion adsorption on the activated carbon may be chemical adsorption or ion exchange [38-40]. The K_2 values showed that Pb^{2+} ions had the highest adsorption capacity and Zn^{2+} the lowest. Thus the trend $Pb^{2+} > Cd^{2+} > Zn^{2+}$ in terms of adsorption.

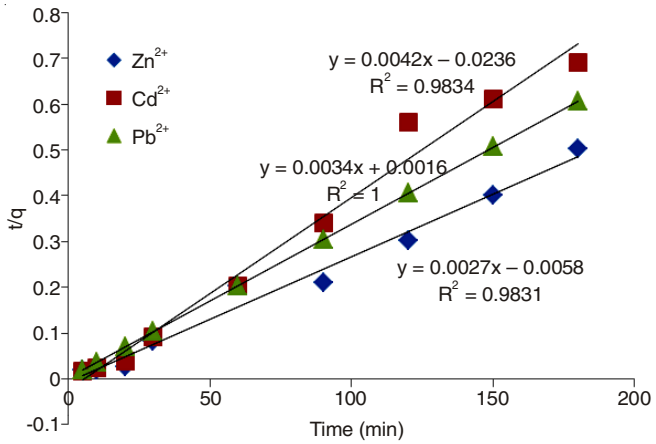

Fig 8. Pseudo-second order kinetics chart for Zn^{2+}, Cd^{2+} and Pb^{2+} ion

TABLE-5
PSEUDO-SECOND ORDER RATE CONSTANTS

Metal ions	q_e exp (mg/g)	h_o (mg/g min^{-1})	q_e cal (mg/g)	R^2
Zn^{2+}	299.11	58.82	301.1	0.981
Pb^{2+}	296.57	999.8	313.3	1.000
Cd^{2+}	299.90	334.2	333.3	0.988

Effect of initial metal ion concentration: Batch adsorption experiments were carried out using various concentrations of the three metal ions ranging from 100 to 500 mg/L at pH 6 and adsorption temperature of 30 °C. The adsorption efficiency was observed to have increased with increased metal ion concentration for the three metal ions (Fig. 9). This behaviour has been ascribed to the availability of more metal ions to be adsorbed at higher concentration. Similar observation have been reported in the literature [12,40].

Adsorption isotherm studies: The experimental data for the adsorption of Pb^{2+}, Zn^{2+} and Cd^{2+} was modelled using the Langmuir and Freudlich adsorption isotherms.

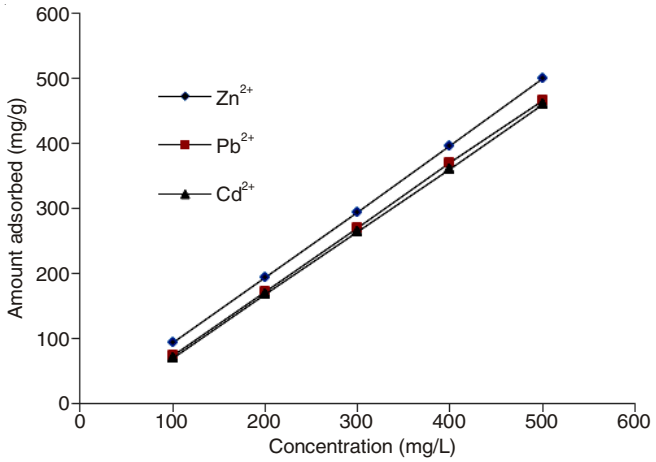

Fig. 9. Graph of amount adsorbed at different concentrations

Langmuir isotherm model: The linear Langmuir isotherm allows the calculation of adsorption capacities and Langmuir constants using the eqns. 7 and 8, respectively.

$$\frac{C_{eq}}{q} = \frac{1}{q_{max}K_L} + \frac{C_{eq}}{q_{max}} \quad (7)$$

$$R_L = \frac{1}{1+K_L C_o} \quad (8)$$

where C_{eq} is the concentration of metal ions at equilibrium (mg/L), q_e is the amount of metal ions adsorbed at equilibrium (mg/g), q_{max} is the maximum adsorption capacity (mg/g) and K_L is the Langmuir isotherm constant related to the energy of adsorption (mg/L). Linear plots of C_{eq}/q against C_{eq} were used to calculate the parameters of the Langmuir isotherm by means of linear regression equations. The q_{max} and K_L were obtained from the slope and intercept of the plots, respectively. The linear Langmuir isotherm parameters are shown in Table-6. The R_L values are between zero and unity for the three metal ions indicate that the mechanism of sorption of the three metal ions on the breadnut activated carbon adsorbent was favourable [7,41]. However the R_L values for the metal ions followed the trend $Pb^{2+} > Zn^{2+} > Cd^{2+}$ indicating that in a mixed metal ion system, that the Pb^{2+} and Zn^{2+} will compete more favourably for binding sites faster than Cd^{2+}. The observed separation factor indicates that high concentration of Pb^{2+}, Zn^{2+} and Cd^{2+} may not be a limiting factor in the ability of the adsorbent to adsorb these metal ions [6,42]. The sorption capacity q_{max} corresponding to complete monolayer coverage showed that the adsorbent had a mass capacity for Zn^{2+} (58.80 mg/g) less Pb^{2+} (71.42 mg/g) and Cd^{2+} (100 mg/g). Table-7 compares q_{max} values for our adsorbent and other closely related adsorbents that has been used for metal ion sequestration. The Langmuir adsorption constant K_L which is related to the apparent energy of adsorption for Cd^{2+} (2.2×10^{-2}) was greater than the values for Zn^{2+} (1.72×10^{-2}) and Pb^{2+} (1.36×10^{-2}) which indicates that the energy for adsorption may be more favourable for Cd^{2+} than $Pb^{2+}$and Zn^{2+} [43].

Freundlich isotherm model: The Freundlich isotherm was chosen to estimate the adsorption intensity of the adsorbent towards the adsorbate. It is represented by eqn. 9:

$$q = K_F C_{eq}^{\frac{i}{n}} \quad (9)$$

where C_{eq} is the equilibrium concentration (mg/L), q is the amount of ion adsorbed (mg/g) and K_F and n are constants incorporating all parameters affecting the adsorption process such as adsorption capacity and intensity, respectively. A linear form of the Freundlich adsorption isotherm [44] was used to evaluate the adsorption data and is represented by eqn. 10:

$$\ln q = \ln K_F + \frac{1}{n}\ln C_{eq} \quad (10)$$

TABLE-6
LANGMUIR AND FREUDLICH CONSTANTS FOR THE ADSORPTION OF Zn^{2+}, Pb^{2+} AND Cd^{2+} IONS

Metal ions	Langmuir constants				Freudlich constants		
	R_L	q (mg/g)	K_L	R^2	1/n	K_F	R^2
Zn^{2+}	0.105	58.80	1.70×10^{-2}	0.720	6.740	1.86×10^{2}	0.764
Pb^{2+}	0.128	71.42	1.36×10^{-2}	0.997	5.880	3.49×10^{2}	0.926
Cd^{2+}	0.083	100.00	2.20×10^{-2}	0.688	5.478	3.09×10^{2}	0.898

TABLE-7
COMPARISON OF ADSORPTION CAPACITIES OF OUR ADSORBENT WITH OTHER ADSORBENTS FROM NATURAL SOURCES

Adsorbent	Metal ions	Adsorption capacity (mg/g)	Ref.
Sugar baggase	Zn(II)	105.26	[48]
Saw dust.	Zn(II)	80.00	[48]
Spirogyra Spp	Pb(II)	90.91	[49]
Cladophora Spp	Pb(II)	46.51	[49]
Fluted pumpkin	Pb(II)	13.70	[50]
Rice husk	Cd(II)	8.58	[51]
	Pb(II)	120.48	
Peanut Husk	Pb(II)	29.14	[52]
Cassava tuber waste	Cd (II)	26.3	[53]
	Zn(II)	83.3	
Jute fibres	Zn(II0	5.95	[54]
Spent grain	Pb(II)	35.5	[55]
Corn cob	Cd(II)	19.3	[56]
Water hyacynth	Cd(II)	70.3	[57]
Pleurotus ostreatus	Zn(II)	3.22	[6]
Cocoa husk		236.16	[58]
Breadfruit nut shell	Pb(II)	71.42	Present work
	Cd(II)	100	
	Zn(II)	58.80	

The values of K_F and n calculated from the intercepts and slopes of the Freundlich plots are given in Table-6. It has been reported that adsorption is favourable for values of $n < 1$ and $1 < n < 2$ [25,45]. The Freundlich equation frequently gives an adequate description of adsorption data over a restricted range of concentrations, even though it is not based on a theoretical background [15, 46]. Apart from a homogenous surface, Freundlich equation is also suitable for a highly heterogeneous surface and an adsorption isotherm lacking a plateau [33]. The values of the Freundlich constants shown in Table-6 indicate that the Freundlich isotherm parameter n which measures adsorption intensity of metal ions on biomass was found to be less than unity for the three metal ions indicating a favourable adsorption [45,47]. This also implies that significant adsorption may take place even at high metal ion concentration [43]. The higher value of 1/n of Zn^{2+} (6.74) in relation to Pb^{2+} (5.880) and Cd^{2+} (5.470) suggest preferential sorption of Zn^{2+} probably due to its smaller ionic radius.

Coefficients of determination: The regression coefficients of determination (R^2) values from the linearization of the two isotherm models are also listed in Table-5. The Langmuir isotherm model provided a good platform for the sorption of Pb^{2+} while the sorption of Zn^{2+} and Cd^{2+} were better fitted to the Freundlich isotherm model.

Conclusions

The application of waste materials from agricultural residues as economical substitutes for commercial activated carbon has been investigated in this study and the experimental results demonstrate the effectiveness of breadnut activated carbon in removing heavy metals from aqueous solution. The Langmuir and Freundlich adsorption models were employed to interpret the adsorption data, while the Largergren pseudo first and second order rate equations were used to investigate the kinetics and mechanism of the sorption process. The following conclusions can be made from this study.

• The efficiency of heavy metal adsorption onto breadnut activated carbon was significantly high reaching up to 87.22 %, 89.68 and 86.39 % Zn^{2+}, $Pb^{2+}$and Cd^{2+} ions, respectively. The amount of metal ion adsorbed was found to increase with increase in contact time, attaining equilibrium at 150 min.

• The uptake capacity of the metal ions onto the adsorbents was found to be dependent on pH of the metal ion solution, adsorbent loading, concentration of metal ion solution and temperature of adsorption.

• The results from the equilibrium sorption experiments indicates that the sorption data for Pb^{2+} ion onto breadnut activated carbon fitted into the Langmuir adsorption isotherm model denoting monolayer adsorption while the data for Zn^{2+} and Cd^{2+} ions was better fitted to the Freundlich adsorption isotherm model indicating multilayer adsorption.

The kinetic studies revealed that the adsorption process for Zn^{2+}, Pb^{2+} and Cd^{2+} ions was consistent with the pseudo-second order rate equation.

ACKNOWLEDGEMENTS

The authors are grateful to Material Engineering Laboratory, University of Waikato, Hamilton, New Zealand for the SEM, EDX and Surface area measurements. The authors also acknowledge to University of Nigeria Nsukka and Tertiary Education Trust Fund Nigeria (TETFUND) for financial support.

REFERENCES

1. O. Amuda, A. Giwa and I. Bello, *Biochem. Eng. J.*, **36**, 174 (2007).
2. H.I. Abdel-Shafy, *Environ. Manage. Health*, **7**, 28 (1996).
3. M. Menkiti and O. Onukwuli, *AIChE J.*, **58**, 1303 (2012).
4. O. Amuda and A. Ibrahim, *Afr. J. Biotechnol.*, **5**, 1483 (2006).
5. M.C. Menkiti, P.M. Ejikeme, O.D. Onukwuli, M.C. Aneke, V.I. Ugonabo and N.U. Menkiti, *J. Chinese Adv. Mater. Soc.*, **3**, 233 (2015).
6. A. Javaid, R. Bajwa, U. Shafique and J. Anwar, *Biomass Bioenergy*, **35**, 1675 (2011).
7. S. Odoemelam, C. Iroh and J. Igwe, *Research J. Appl. Sci.*, **6**, 44 (2011).
8. J. Igwe and A. Abia, *Int. J. Phys. Sci.*, **2**, 119 (2007).
9. K. Kadirvelu, M. Kavipriya, C. Karthika, M. Radhika, N. Vennilamani and S. Pattabhi, *Bioresour. Technol.*, **87**, 129 (2003).
10. D. Mohan and K.P. Singh, *Water Res.*, **36**, 2304 (2002).
11. O. Okpareke, I.I. Agha and P. Ejikeme, *J. Chem. Soc. Nigeria*, **35**, 94 (2010).
12. K. Kadirvelu and C. Namasivayam, *Environ. Technol.*, **21**, 1091 (2000).
13. V.K. Gupta and I. Ali, *J. Colloid Interf. Sci.*, **271**, 321 (2004).
14. H. Cho, D. Oh and K. Kim, *J. Hazard. Mater.*, **127**, 187 (2005).
15. N. Narkis and B. Ben-David, *Water Res.*, **19**, 815 (1985).
16. M. Machida, R. Yamazaki, M. Aikawa and H. Tatsumoto, *Sep. Purif. Technol.*, **46**, 88 (2005).
17. S. Mohan and R. Gandhimathi, *J. Hazard. Mater.*, **169**, 351 (2009).
18. A.S. Krishna Kumar, S.-J. Jiang and W.-L. Tseng, *J. Mater. Chem. A*, **3**, 7044 (2015).
19. Y. Ho, J. Porter and G. McKay, *Water Air Soil Pollut.*, **141**, 1 (2002).
20. N.P. Roeges, A Guide to the Complete Interpretation Infrared Spectra Organic Structures, Wiley (1994).
21. B. Stuart, Infrared spectroscopy, Wiley Online Library (2005).
22. K.S. Hui, C.Y.H. Chao and S.C. Kot, *J. Hazard. Mater.*, **127**, 89 (2005).
23. C. Pevida, M.G. Plaza, B. Arias, J. Fermoso, F. Rubiera and J.J. Pis, *Appl. Surf. Sci.*, **254**, 7165 (2008).
24. Z. Li, Y. Ge and L. Wan, *J. Hazard. Mater.*, **285**, 77 (2015).
25. J.C. Moreno-Piraján, V.S. Garcia-Cuello and L. Giraldo, *Adsorption*, **17**, 505 (2011).
26. F. Çolak, A. Olgun, N. Atar and D. Yazicioglu, *J. Ind. Eng. Chem.*, **19**, 863 (2013).
27. N. Abdel-Ghani, M. Hefny and G.A. El-Chaghaby, *Int. J. Environ. Sci. Technol.*, **4**, 67 (2007).

28. B. Bayat, *J. Hazard. Mater.*, **95**, 251 (2002).
29. M.M. Dávila-Jiménez, M.P. Elizalde-González and V. Hernández-Montoya, *Bioresour. Technol.*, **100**, 6199 (2009).
30. F. Di Natale, A. Erto, A. Lancia and D. Musmarra, *Water Res.*, **42**, 2007 (2008).
31. F. Di Natale, A. Erto, A. Lancia and D. Musmarra, *J. Hazard. Mater.*, **192**, 1842 (2011).
32. F. Di Natale, A. Erto, A. Lancia and D. Musmarra, *J. Hazard. Mater.*, **281**, 47 (2015).
33. A.B. Albadarin, C. Mangwandi, A.H. Al-Muhtaseb, G.M. Walker, S.J. Allen and M.N.M. Ahmad, *Chem. Eng. J.*, **179**, 193 (2012).
34. J. Hu, G. Chen and I.M. Lo, *Water Res.*, **39**, 4528 (2005).
35. C. Sing and J. Yu, *Water Res.*, **32**, 2746 (1998).
36. Y.-S. Ho and G. McKay, *Chem. Eng. J.*, **70**, 115 (1998).
37. V. Lenoble, O. Bouras, V. Deluchat, B. Serpaud and J.-C. Bollinger, *J. Colloid Interf. Sci.*, **255**, 52 (2002).
38. K. Chong and B. Volesky, *Biotechnol. Bioeng.*, **47**, 451 (1995).
39. B. Volesky and Z. Holan, *Biotechnol. Prog.*, **11**, 235 (1995).
40. S. Sana, R. Roostaazad and S. Yaghmaei, *Iran. J. Chem. Chem. Eng.*, **34**, 60 (2015).
41. Y.-S. Ho and G. McKay, *Process Saf. Environ. Prot.*, **76**, 183 (1998).
42. Z. Aksu, *Process Biochem.*, **40**, 997 (2005).
43. J.M. Horsfall and A.I. Spiff, *Electron. J. Biotechnol.*, **8**, 43 (2005).
44. M. Chaudhary, *Pharm. Res.*, **2**, 30 (2011).
45. S.S. Shukla, L.J. Yu, K.L. Dorris and A. Shukla, *J. Hazard. Mater.*, **121**, 243 (2005).
46. V. Ravindran, M.R. Stevens, B.N. Badriyha and M. Pirbazari, *AIChE J.*, **45**, 1135 (1999).
47. R. Say, A. Denizli and M.Y. Arica, *Bioresour. Technol.*, **76**, 67 (2001).
48. F.V. Pereira, L.V.A. Gurgel and L.F. Gil, *J. Hazard. Mater.*, **176**, 856 (2010).
49. Y.-C. Lee and S.-P. Chang, *Bioresour. Technol.*, **102**, 5297 (2011).
50. A. Okoye, P. Ejikeme and O. Onukwuli, *Int. J. Environ. Sci. Technol.*, **7**, 793 (2010).
51. K. Wong, C. Lee, K. Low and M. Haron, *Chemosphere*, **50**, 23 (2003).
52. Q. Li, J. Zhai, W. Zhang, M. Wang and J. Zhou, *J. Hazard. Mater.*, **141**, 163 (2007).
53. M. Horsfall Jr., A. Abia and A. Spiff, *Bioresour. Technol.*, **97**, 283 (2006).
54. S. Shukla and R.S. Pai, *Bioresour. Technol.*, **96**, 1430 (2005).
55. K. Low, C. Lee and S. Liew, *Process Biochem.*, **36**, 59 (2000).
56. R. Leyva-Ramos, L. Bernal-Jacome and I. Acosta-Rodriguez, *Sep. Purif. Technol.*, **45**, 41 (2005).
57. F. Zhang, X. Wang, D. Yin, B. Peng, C. Tan, Y. Liu, X. Tan and S. Wu, *J. Environ. Manage.*, **153**, 68 (2015).
58. A.O. Aderonke, B.A. Abimbola, E. Ifeanyi, S.A. Omotayo, S.A. Oluwagbemiga and W.M. Oladotun, *Afr. J. Pure Appl. Chem.*, **8**, 147 (2014).